Langmuir

ARTICLE

pubs.acs.org/Langmuir

Layer-by-Layer Self-Assembly of Single-Walled Carbon Nanotubes with Amine-Functionalized Weak Polyelectrolytes for Electrochemically Tunable pH Sensitivity

Dongjin Lee and Tianhong Cui*

Department of Mechanical Engineering, University of Minnesota, 111 Church St. S.E., Minneapolis, Minnesota 55455, United States

ABSTRACT: The layer-by-layer (LbL) assembly of carboxylated single-walled carbon nanotubes (SWCNT) is demonstrated to tune the electrochemical pH sensitivity of thin-film devices. The positively charged amine containing weak polyelectrolyte (wPE) is used as a counter species to control the proximal ions. The LbL assembly process is monitored by the quartz crystal microbalance, which results in the linear growth of a multilayer. The amount adsorbed is strongly dependent on the surface charge of previously deposited species. However, the thickness of the multilayer is determined by both the amount adsorbed and the coiling of polyelectrolyte chains. Indeed, electrical and structural characteristics of the (wPE/SWCNT) multilayer thin film are obtained according to the acid dissociation constants of amino groups in wPE. The electrochemical pH sensitivity in the physiological range demonstrates the effects of both charge carrier doping/trapping and proximal ions on the conductance of the SWCNT multilayer. Although doping/trapping shows the decreasing conductance, the proximal ion effect reveals the increasing conductance with pH in the basic region as a result of the p-type semiconducting nature of SWCNTs and the ability of wPE to capture hydrogen ions. This work sheds light on the applicability of nanostructured and/or engineered functional thin films of SWCNTs as chemical and biological sensors.

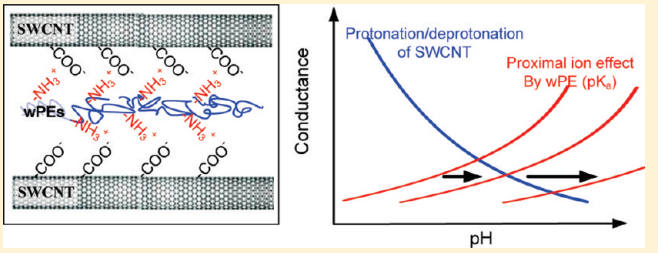

INTRODUCTION

Since their discovery,[1] carbon nanotubes (CNT's) have attracted a great amount of interest in both academic and industrial sectors for a variety of potential applications in chemical[2] and biological sensors,[3] actuators,[4] nanoelectronics,[5] nanoelectromechanical systems (NEMS),[6] and atomic force microscopy.[7] To take advantage of excellent mechanical, electrical, and optical properties, CNTs should be integrated into existing devices or matrix materials as active structure, electrical conductor/insulator, sensor, actuator, and light absorbing/emitting components. A CNT thin film has been fabricated as functional structures in sensors,[8] flexible displays, solar cells,[9] and transistors by solution-based methods such as Langmuir−Blodgett (LB) films,[10,11] spraying,[8,9] spin coating,[9] and electrostatic layer-by-layer (LbL) assembly. Deposition over a large area with patterning capability using microfabrication technologies is needed for high-throughput device fabrication. Furthermore, the controllability of CNT films in terms of the structure, thickness, and orientation is a key to tailoring film properties and functionality. For example, the density and thickness of CNT thin films are important parameters in controlling the transparency and electrical conductance. LbL assembly has attracted a great amount of attention because of its molecular-level thickness controllability,[12] thermodynamic stability, versatility, simplicity, and low cost. It can easily tune the internal structure of a thin film by altering the pairing species, charge density, ionic strength, and solution pH in cases of weak electrolytes. The LbL self-assembly of CNTs has been highlighted as a postgrowth assembly method for incorporating CNTs into existing devices without segregation.[13] LbL-assembled CNTs have been used primarily as sensors[14−16] and actuators.[17]

One mainstream CNT application is chemical and biological sensors to take advantage of novel electrochemical transduction properties that resulted from interactions among CNTs and adjacent molecules. The study of the electrochemical properties[18] triggered significant electrochemical biosensing applications capable of detecting or monitoring specific biomolecules. Among the extensive chemical and biological sensing applications reported, pH sensing is of great importance in scientific research and clinics because it determines the solubility, charge on biomolecules, and equilibrium of biochemical reactions. For example, cancer cells tend to breed in acidic environments whereas normal human blood has a pH of 7.35.[18] Mitogenic stimulation on cells leads to ionic concentration changes, so the pH in cytoplasm is an indication of the progression to DNA synthesis after fertilization.[19] pH detection and monitoring, consequently, provide biologically meaningful information. CNTs comply with such a strong demand for a miniaturized ion-sensing probe to monitor the pH in situ in a single cell. Furthermore, there are biochemical reactions accompanying a pH change by which the concentration of substrate molecules is traced. Indeed, the study and engineering of the pH sensitivity of CNTs are important to electrochemical sensing application.

Received: November 29, 2010
Revised: January 22, 2011
Published: February 23, 2011

Combined with the extremely sensitive electronic properties of CNTs, CNT pH sensors were reported.[8,20−24] In particular, microfabricated MEMS-based devices[8,20,24] used pristine CNTs, where the conductance of CNT network increased with pH. The authors argued that the changes in an ionic environment of CNTs, mainly hydrogen ions or hydroxyl ions, modulated the charge-carrier transfer characteristics, thereby yielding the pH-dependent conductance or current at a fixed bias voltage. However, we previously demonstrated that a carboxylated CNT film exhibited the opposite conductance behavior, showing decreasing conductance with increasing pH.[25] In particular, the exponential relation between current and pH substantiated the effect of protonation/depronation on the conductance of CNT films. It was postulated that protonation/deprotonation played the role of charge-carrier doping/trapping,[25] which made it possible to engineer the pH sensitivity of CNTs. However, the effect of proximal ions on the conductance of a CNT network or individual CNTs still existed, which meant that protonation/deprotonation played a dominant role in the pH sensitivity of carboxylated CNT thin films. Strong polyelectrolyte poly(diallyldimethylammonium chloride) (PDDA) has no pH-sensitive side groups, so the effect of proximal ion on the conductance was expected to be the same in various pH buffers. Even though the pH sensing mechanism in pristine CNTs was explained by the proximal ion effect, no experimental effort has been reported to control the number of ions in the vicinity of CNTs in order to tune the pH sensitivity.

In this article, carboxylated SWCNTs were LbL self-assembled with weak polyelectrolyte (wPE) possessing amine-functionalized groups with different acid dissociation constants (K_a) that control the number of proximal H^+ and OH^-. In this way, the effect of proximal ions on the conductance changes of CNT thin films is systematically studied. We show that the internal structure of a CNT thin film fabricated by versatile LbL assembly is an important parameter in tuning the electrical and/or electrochemical properties. The PEs containing amine groups are weakly charged polycations whose charge is affected by the pH of the dispersant. The wPEs used here are chitosan, polyallylamine hydrochloride, and poly-L-lysine. The wPEs are interlaid between SWCNT layers using the LbL scheme. A quartz crystal microbalance, a surface profiler, and a semiconductor parameter analyzer are used to estimate the interal structure in LbL thin films. The pH sensitivity of five bilayers of each wPE is characterized using a chemoresistor scheme, where two terminals are used for $I-V$ measurements. Their performance will be discussed on the basis of the kind of interlaid wPEs in terms of the pK_a, structure, and adsorption phenomena. Furthermore, the results will be compared with $(PDDA/SWCNT)_5$ devices as a standard. The pH sensitivity in the physiological range demonstrates the effect of proximal ions on the conductance of CNT thin films as a result of the electronic nature of SWCNTs and the ability to capture hydrogen ions in wPEs. This work sheds light on the applicability of nanostructured and/or functionalized CNTs with various functional groups as pH sensors and biological sensors.

EXPERIMENTAL SECTION

Materials. Single-walled carbon nanotubes (SWCNTs, 90% purity of SWCNTs and 95% purity of CNTs, diameter 1−2 nm, length 5−30 μm, SSA 300−380 m^2/g) were purchased from Nanostructured & Amorphous Materials, Inc. SWCNTs (0.5 g) were chemically functionalized in a 3:1 mixture of concentrated sulfuric acid (150 mL, H_2SO_4) and nitric acid (50 mL, HNO_3) at 110 °C for an hour,[26] followed by 5-fold dilution into water and vacuum filtration with a pore size of 0.22 μm. After being rinsed with deionized water (DW) several times until the pH approached 5, the functionalized SWCNTs were harvested and dispersed into 500 mL of fresh DW with the aid of sonication for an hour. Subsequently, the SWCNT solution was centrifuged at a speed of 4500g (5000 rpm, Eppendorf centrifuge 5804) for 20 min to eliminate aggregates and bundles. The supernatant was carefully decanted, and the precipitates were discarded. The final concentration of the SWCNT solution was 0.6 mg/mL. The pH of the aqueous SWCNT dispersion was 5. Reflective Fourier transform infrared spectroscopy (FTIR, Nicolet Magna IR 750) in a drop-cast film showed a strong C═O stretching vibration, which is an indication of carboxylic groups resulting from chemical functionalization.

Poly(diallyldimethyammonium chloride) (PDDA, M_w = 200−350K, Sigma-Aldrich) and poly(styrene sulfonate) (PSS, M_w = 70K, Sigma-Aldrich) were used to build up a precursor layer in order to enhance the surface charge in the initial stage of LbL assembly. The aqueous concentrations of PDDA and PSS used were 1.4 and 0.3 wt %, respectively, with 0.5 M sodium chloride (NaCl). The wPE solutions were prepared as follows. Chitosan (Chit, 75−85% deacetylated, Sigma-Aldrich) in a 0.1 wt % aqueous solution was prepared using sodium acetate buffer (pH 5.2, 30 mM) to make sure that the chitosan polymer had enough positive charge to be a stable solution. Poly(allylamine hydrochloride) (M_w= ∼56K, PAH) and poly-L-lysine (PLL, M_w = 70−150K) were obtained from Sigma-Aldrich. PAH was dissolved in DW to produce a concentration of 0.3 wt % so that the final solution yielded a pH of 6.4. A 0.1 wt % PLL solution at pH 9.0 was used without further treatment.

Standard pH buffer solutions used for the pH-sensitivity study were formulated using sodium phosphates. A mixture of phosphate monobasic monohydrate ($NaH_2PO_4 \cdot H_2O$, Mallinckrodt Baker, Inc.) and phosphate dibasic heptahydrate ($Na_2HPO_4 \cdot 7H_2O$, Mallinckrodt Baker, Inc.) was used to produce a pH in the physiological range with a buffering power of 80 mM.

Device Fabrication and Layer-by-Layer Assembly. Chromium (Cr, 250 Å) and gold (Au, 1000 Å) were electron-beam evaporated on a standard 4 in. silicon (Si) wafer with 2-μm-thick silicon dioxide (SiO_2) and patterned for source and drain electrodes. Another lithographic technique was used to fabricate a photoresist window area through which the LbL film was assembled onto the conducting channel. It protected the measuring pads and eliminated a possible direct electrochemical reaction between the pH buffer and Cr/Au electrode covered with a self-assembled SWCNT film in an area other than the conducting channel. Oxygen (O_2) plasma was used at a power of 100 W for 1 min with an O_2 flow rate of 100 sccm to remove the residual photoresist completely in the opening window as well as to make the exposed surface hydrophilic, which is beneficial to the subsequent LbL assembly. The thin-film structure of $[(PDDA\ (10\ min)/PSS\ (10\ min)]_2 + [(wPE\ (10\ min)\ /SWCNT\ (15\ min)]_5$ was assembled, followed by lift off.

Quartz Crystal Microbalance (QCM) Measurement. The LbL process was monitored with a quartz crystal microbalance (R-QCM, Maxtek Inc.) at room temperature to evaluate the number of wPEs and SWCNTs adsorbed and correlate it to the surface charge of the previously adsorbed species. The crystal that was used was an AT-cut 9 MHz crystal with an active oscillation area of 0.34 cm^2. Prior to the QCM test, crystals were covered with $(PDDA/PSS)_2$ and one additional layer of wPE. The frequency of the crystal at this point in the dry state was set to zero. Then the crystal was dipped into wPE or SWCNT solution for a given dipping time, removed, rinsed thoroughly with DW, and dried in a stream of nitrogen. The frequency of the QCM crystal was recorded. The frequency shift corresponded to the amount of adsorbed substances by the Sauerbrey equation.

Electrical Characterization. The electrical resistance of devices was measured with semiconductor parameter analyzer (HP4145B). A bias voltage is applied to the drain electrode with the source electrode grounded, and the current (I) flowing through the SWCNT thin film is measured. The device demonstrated a linear current−voltage relationship in the air. For electrical characterization in an aqueous solution, the device was dipped into DW for an hour to reduce the drift in the sample solution and dried with a stream of nitrogen prior to use. For the pH-sensitivity test, 250 μL of a pH buffer was added to the device surface and incubated for 1 min, followed by $I-V$ measurement. The device surface was rinsed with DW three times after the old buffer was removed. At the same bias voltage, different current levels are found depending on the pH buffer primarily because of the mutation in the electrical properties of the thin film. pH-sensitivity tests were performed for five devices with each wPE, and the currents were normalized with that for the pH 5 buffer.

Thickness Measurement. The micropattern of $(wPE/SWCNT)_5$ was used to measure the thickness of a thin film with a surface profiler (P-16, KLA-Tencor) at a force of 19.6 μN and a scanning speed of 20 μm/s. The step heights on 12 different spots were averaged and compared.

RESULTS AND DISCUSSION

The carboxylated SWCNTs were LbL assembled alternately with positively charged polyelectrolytes containing amine groups as shown in Figure 1. Protonation/deprotonation occurs on carboxylic groups in SWCNTs, which can be considered the direct doping/undoping of charge carriers in SWCNTs. Eventually, the deprotonation of carboxylic groups induced the exponentially decreasing conductance of SWCNT thin films with increasing pH. The wPEs used in this study were chitosan (Chit), poly(allylamine hydrochloride) (PAH) and poly-L-lysine (PLL), and their molecular structures are shown in Figure 1b. The wPEs have the positive charge of $-NH_3^+$ in the case where it is subjected to pH below the pK_a and the neutral charge of $-NH_2$ at pH above the pK_a, so it is stable in an acidic environment as a colloid, which is essential for LbL assembly. The pK_a values of amino group of Chit, PAH, and PLL were reported to be 6.5, 8.5, and 10.5.[27] In addition to that on SWCNTs, protonation/deprotonation happens on amine group in wPEs as illustrated in Figure 1a because they have different acid dissociation constants (K_a) as summarized in Table 1. Therefore, the interlaid wPEs have different capacities for holding hydrogen or hydroxyl ions depending on K_a,[27] which influences the conductance of the SWCNT layer. This pH-gating behavior was observed previously, where an increase in pH corresponds to a negative shift in the gate voltage from the conventional semiconductor point of view. This fact also resulted in increased conductance in pristine SWCNT films. As a result, the protonation/deprotonation on SWCNTs and pH gating have opposite effects on the conductance of SWCNT thin films. Consequently, we show the different sensitivity by employing wPEs with different acid constants of side amine groups.

The fabricated SWCNT multilayer thin-film devices are shown in Figure 2. The size of the devices is 1 cm × 1 cm as shown in Figure 2a, and the SWCNT multilayer was confined in the conducting channel as shown in Figure 2b between the drain and source electrodes. The conducting channel dimensions were a length of 10 μm and a width of 1 mm. The surface of the SWCNT thin film was characterized with field emission gun−scanning electron microscopy (FE-SEM, Jeol 6700), and the image of $(PLL/SWCNT)_5$ is shown in Figure 2c. The individual

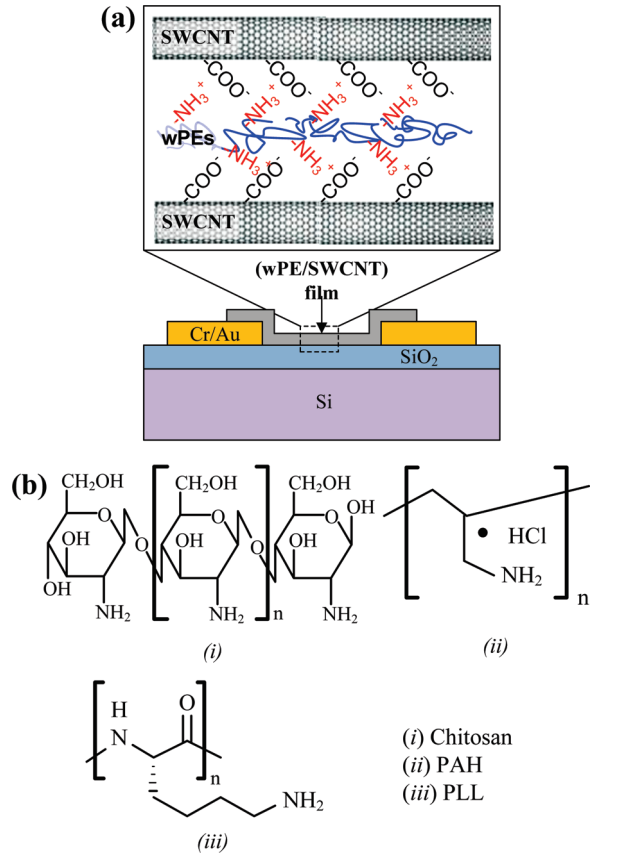

Figure 1. Layer-by-layer-assembled carbon nanotube thin-film device with weak polyelectrolyte (wPEs) as pairing species: (a) schematic of a device with a side functional group of −COOH on SWCNT and $-NH_3^+$ on wPEs and (b) the molecular structure of the wPEs used, where the different pK_a of $-NH_3^+$ on wPEs influences the pH sensitivity of the multilayered film.

CNTs and bundles and a random network of these are clearly observed. However, the film morphology did not demonstrate a significant difference among $(PDDA/SWCNT)_5$, $(Chit/SWCNT)_5$, and $(PAH/SWCNT)_5$ devices.

The result of the QCM measurement of multilayer growth is shown in Figure 3, demonstrating significant differences among the three wPEs used. The frequency decreases with the number of layers assembled as shown in Figure 3a. It is also observed that the SWCNT multilayer grows linearly with wPEs as seen in LbL assembly with a strong PE, PDDA.[28] Furthermore, the growth rate is dependent on the species of wPEs presumably because of the surface charge. The growth rate of (PLL/SWCNT) is the greatest of the three wPEs tested, being almost 2 times greater than that of (Chit/SWCNT). The charge and/or conformation of wPE chains may influence the growth rate.[29] The average frequency shift for wPEs and SWCNTs is depicted in Figure 3b with the standard deviation as an error bar. Although the amount of wPEs increases slightly, that of SWCNTs increases significantly following the order of Chit, PAH, and PLL, approaching the amount deposited in the LbL process of (PDDA/SWCNT). Smaller amounts of wPE and SWCNTs are deposited because of the weak charge on the wPE.

On the basis of the fact that LbL assembly fully covers the crystal surface as sustained by SEM images in Figure 2c, the

dx.doi.org/10.1021/la1047547 |Langmuir 2011, 27, 3348–3354

Table 1. Mass Assembled per Unit Area of wPEs and SWCNT with pH and the Acid Dissociation Constant (pK_a)

				mass assembled (ng/cm^2)				
PE	solution pH	charge	pK_a of amino group[27]	PE	SWCNT	bilayer	PE surface charge in SWCNT solution ($pK_{a,\ PE} - pH_{CNT}$)	SWCNT surface charge in wPE solution ($pK_{a,\ CNT} - pH_{PE}$)
Chit	5.2	weak polycation	6.5	214.4	465.2	679.6	1.5	−0.7
PAH	6.4	weak polycation	8.5	239.2	675.1	914.4	3.5	−1.9
PLL	9.0	weak polycation	10.5	284.5	935.2	1219.7	5.5	−4.5
PDDA[28]		strong polycation		337.6	1008.3	1345.9		

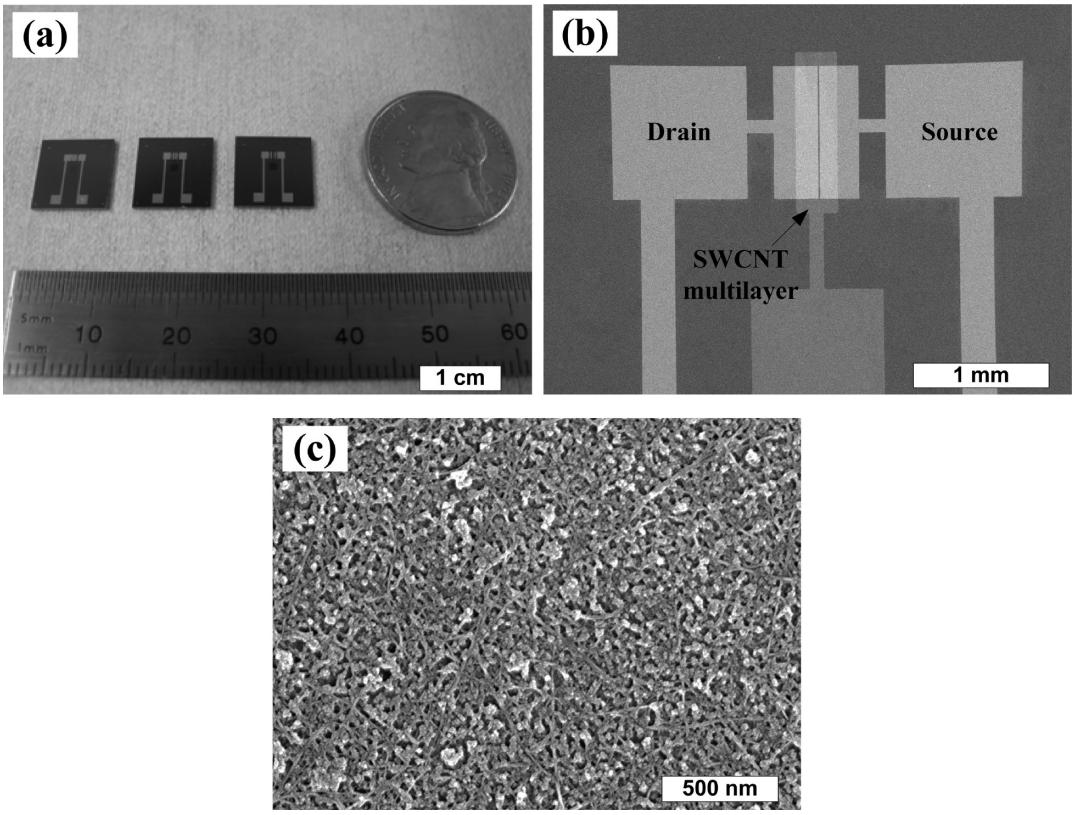

Figure 2. Fabricated SWCNT multilayer with different wPE's: (a) 1 cm ×1 cm individual pH-sensing device, (b) electrode pattern with SWCNTs multilayered with wPEs, and (c) an SEM image of an LbL film, where the difference in morphology was not observed among three different wPE's.

average frequency shifts correspond to the mass adsorbed by the Sauerbrey equation as follows

$$\Delta f = -C_f \Delta m_s$$

where Δf is the frequency shift in Hz, C_f is the sensitivity factor of the crystal used (0.181 Hz·cm^2·ng^{-1} for a 9 MHz AT cut crystal), and Δm_s is the mass adsorbed per unit area in ng·cm^{-2}. The adsorbed mass per unit area is summarized in Table 1. Furthermore, the mass assembled is correlated with the acid dissociation constants (pK_a) and solution pH. The pH of wPE solutions was designated with respect to the way in which the pH is lower than the pK_a to make sure that wPEs are stable in aqueous solution. The pK_a of SWCNTs is constant and is assumed to be 4.5[30] in the following consideration. During SWCNT assembly, the surface of the substrate was covered with wPEs whose charges are dependent on the pH of the SWCNT solution. The amino groups on wPEs are subject to the pH of the SWCNT solution, which is considered to be constant. By the Henderson−Hasselbach equation, the ratio of protonated to deprotonated weak acid is determined by the pK_a value of the protonated weak acid. Therefore, the relative surface charge of wPEs in SWCNT solution is defined as the subtraction of the pH of the SWCNT solution from the pK_a value of wPEs: $pK_{a,PE} - pH_{CNT}$. Likewise, SWCNTs are subjected to different pH values of wPE solutions during wPE deposition. Consequently, the charge on the SWCNT-terminated surface is defined as the subtraction of the pH of the wPE from the pK_a of the SWCNT: $pK_{a,CNT} - pH_{PE}$. The pH and pK_a for each wPE along with the relative surface charge of wPEs and SWCNTs in the opposite solutions are summarized in Table 1. The relative surface charge is correlated with the mass assembled and depicted in Figure 4. The amino groups on wPEs are protonated or deprotonated depending on the pH of the SWCNT solution, which corresponds to wPE's

dx.doi.org/10.1021/la1047547 |*Langmuir* 2011, 27, 3348–3354

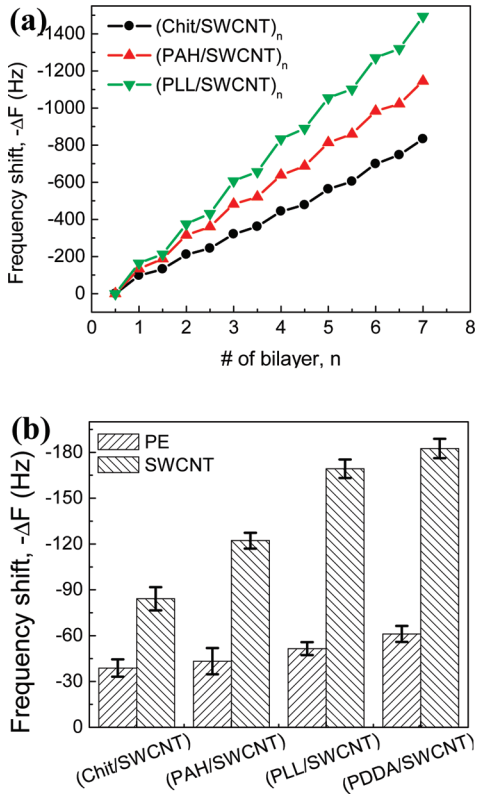

Figure 3. Quartz crystal microbalance (QCM) measurement of (wPE/SWCNT) multilayer growth: (a) monitoring of multilayer growth in the dry state and (b) the average frequency shift for wPEs and SWCNTs in the QCM test with a comparison to strong polyelectrolyte composite (PDDA/SWCNTs). Error bars indicate the standard deviation.

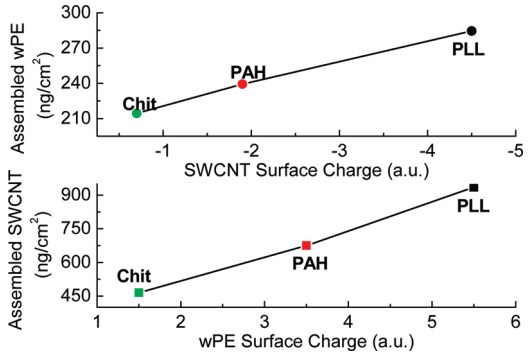

Figure 4. Relationship between assembled mass per unit area and the relative surface charge of previously adsorbed species during LbL assembly. A linear relationship is observed between the charge of the substrate surface and the quantity of oppositely charged species.

surface charge in SWCNT solutions. The amount of SWCNT absorbed is linearly dependent on the relative surface charge of wPEs that was assembled in the previous step of LbL assembly. In the same way, the carboxylic groups on SWCNTs are protonated or deprotonated depending on the pH of the wPE solutions. Therefore, the quantity of wPEs is determined by the relative charge of SWCNTs in wPE solutions with a linear relationship. As a result, the relationship between the quantity of assembled species and the relative surface charge that was

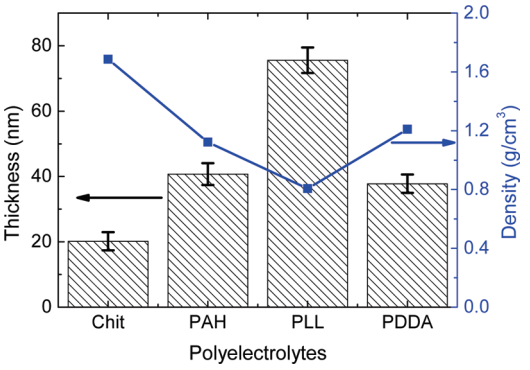

Figure 5. Thickness and density of the (wPE/SWCNT)$_5$ thin film. The thickess was measured using the surface profiler, and the density was calculated on the basis of the mass per unit area and the measured thickness. The error bars stand for the standard deviation.

extracted from the pK_a of previously adsorbed species and the solution pH is linear.

The thickness and density of the (wPE/SWCNT)$_5$ thin film are shown in Figure 5. The thickness was measured using the surface profiler on 12 different spots, where the step height was fabricated. The density of the thin film was calculated by dividing the assembled mass per unit area shown in Figure 4 by the measured thickness. The thickness of the (wPE/SWCNT) thin film is dependent on the quantity of wPEs and SWCNTs assembled and the coiling of polyelectrolytes during LbL assembly. However, it is interesting that the thickness of (PAH/SWNT)$_5$ is comparable to that of (PDDA/SWCNT)$_5$.[28] Even though the quantity of PAH and SWCNT is less than that of (PDDA/SWCNT)$_5$, more coiling of PAH polymer chains is expected because of the weak charge and the absence of sodium chloride that was used in (PDDA/SWCNT)$_5$. Another possibility is that a layer of wPE generates a low density because of its weak charge so that SWCNT penetrates into the sparsely packed wPE layer to some degree in the next step of LbL assembly, resulting in a smaller effective thickness of the SWCNT layer. Furthermore, the weak charge also induces fewer assembled SWCNTs. In this way, (PAH/SWCNT)$_5$ has a comparable thickness to (PDDA/SWCNT)$_5$. Among the three kinds of wPEs used, the thickness of the multilayer seems to be strongly dependent on the quantity of wPEs and SWCNTs. However, the effect of the wPE species is more significant to thickness than the quantity, which results in decreasing density following the order of (Chit/SWCNT)$_5$, (PAH/SWCNT)$_5$, and (PLL/SWCNT)$_5$ and a thicker film in (PLL/SWCNT) than in (PDDA/SWCNT). The thickness of (Chit/SWCNT)$_5$ was half but the thickness of (PLL/SWCNT)$_5$ was almost double compared to that of (PAH/SWCNT)$_5$. The major reason for the doubled thickness in (PLL/SWCNT)$_5$ is the distinctive interlaid PLL layer due to more coiling of the polymer chains inside the film structure and the quantity of PLL and SWCNT assembled. Indeed, the wPEs made their own thin-film structure characteristics.

I−*V* measurement of the SWCNT thin-film devices showed a linear relationship at forward and backward biases at the atmosphere, indicating ohmic contact between the (wPE/SWCNT) multilayer thin film and the metal electrodes. The resistance of devices was calculated at the bias voltage of 0.5 V. Generally, the weak polyelectrolyte devices had 3-fold higher resistance than (PDDA/SWCNT)$_5$ devices, as shown in Figure 6, even though

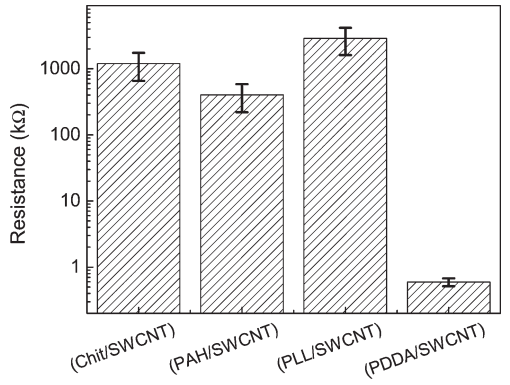

Figure 6. Resistance of $(wPE's/SWCNT)_5$ with a comparison to $(PDDA/SWCNT)_5$ devices: $(wPE's/SWCNT)_5$ shows a 3-fold higher resistance than $(PDDA/SWCNT)_5$ devices because of the reduced electrical contact between neighboring SWCNT layers caused by the coiling of wPE's chain. Error bars denote the standard deviation.

the quantity of SWCNTs assembled is comparable to that in $(PDDA/SWCNT)_5$ devices, which was identified in Figure 3. It is apparent that the electrical conductance of SWCNT devices with wPEs is not dependent solely on the quantity of SWCNTs assembled. For electrical charge carrier transfer, SWCNTs should be in contact with each other in the same layer or a layer of SWCNTs should come in contact with the neighboring SWCNT layers. However, wPE chains tend to be more serpentine than PDDA molecules because of the reduced repulsive force between charged side groups. The thickened wPE layer might hamper the electrical contacts between the consecutive SWCNT layers.

Finally, the pH sensitivity of a SWCNT thin-film possessing wPE's as pairing species was characterized as shown in Figure 7. The schematic of the pH sensitivity test is shown in Figure 7a. After two terminals, the source and drain electrodes were connected to a semiconductor parameter analyzer, a pH buffer was added to the surface of the device, and voltage was applied as in Figure 7b. After $I-V$ curves in the range of 0 to 0.5 V were measured for each standard pH buffer, the currents at a bias voltage of 0.5 V were extracted. Five devices were tested in this way, and the currents were normalized to the one at pH 5 to compare the general behavior of pH sensitivity as shown in Figure 7c. The error denotes the standard deviation. The resistance of the devices plateaued when five bilayers of (wPE/SWCNT) were deposited, which means that additional layers did not strongly influence the resistance of the device. To obtain the maximum effect of the weak polyelectrolyte on the resistance of the devices in a pH buffer, we used five bilayers in this study. Although the normalized current in $(Chit/SWCNT)_5$ decreases slightly and increases after pH 7, those in $(PAH/SWCNT)_5$ and $(PLL/SWCNT)_5$ monotonically decrease. Most of the amino groups in Chit are deprotonated because of their low pK_a value, so the potential in the vicinity of a SWCNT shifts negatively to allow more current in p-type semiconducting nanotubes. However, in the basic region, the normalized current in $(PLL/SWCNT)_5$ is smaller than that in $(PAH/SWCNT)_5$, which suggests a higher sensitivity in the basic region. More amino groups are deprotonated in $(PAH/SWCNT)_5$ than in $(PLL/SWCNT)_5$, leading to a more negative shift in potential that resulted in more current. All $(wPEs/SWCNT)_5$ thin-film devices have their own hydrogen ion holding capability in the side functional amino groups, which influences the conductance of the SWCNT layer. It is significantly changed in the basic region because of the p-type semiconducting SWCNTs because the increase in pH corresponds to the application of a negative gate voltage, resulting in a more conductive channel formed inside the SWCNT layer. It is obvious to see this phenomenon in the pH sensitivity of pristine SWCNTs.[8,20] However, it is noted that carboxylated SWCNTs still have their own pH-responsive conductance induced by charge-carrier doping/trapping,[25] which is assumed to have the same effect in the three kinds of devices tested. This dominates the overall sensitivity, which decreases exponentially with increasing pH. Consequently, a tunable pH sensitivity of the (wPE/SWCNT) multilayer film could be obtained by employing the pairing wPEs with different pK_a values, which could be more controllable by grafting different functional groups onto SWCNTs through other functionalization schemes. For example, in an acidic environment, the protonation/deprotonation of $-COOH$ is dominant because the pK_a of $-COOH$ is less than 7, whereas the pK_a of $-NH_3^+$ plays the primary role of modulating the pH sensitivity in basic solution.

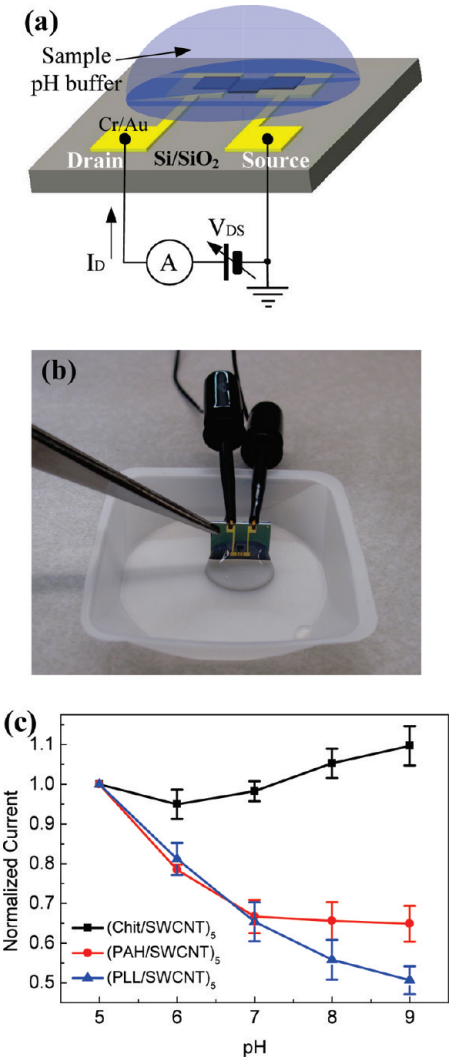

Figure 7. pH-sensitivity testing of a SWCNT thin film with interlaid amine-containing wPE's: (a) electrochemical testing scheme, (b) photograph of electrochemical characterization, and (c) general pH-sensitivity behaviors of $(wPE/SWCNT)_5$ devices. The pH sensitivity is tuned by employing wPE's with different pK_a values.

dx.doi.org/10.1021/la1047547 |*Langmuir* 2011, 27, 3348–3354

CONCLUSIONS

The wPEs with amine functional groups have been used as paring species along with carboxylated SWCNTs in LbL self-assembly, resulting in different internal structures from that of the (PDDA/SWCNT) multilayer. The multilayer grew linearly with the dipping time, and the quantity of the adsorbed species was correlated with the surface charge of the opposite species deposited in a previous step of LbL self-assembly. It is proven to be linear with respect to the relative surface charge. However, the thickness of multilayered film is dependent on both the quantity of species assembled and the coiling of the wPE chain. (wPE/SWCNT) had a 3-fold higher resistance than (PDDA/SWCNT) devices because of the prevention of electrical contact among neighboring SWCNT layers caused by a thick interlaid wPE layer. Finally, a pH response with a different trend in sensitivity due to the p-type semiconducting SWCNTs was exhibited. Indeed, the presence of pH-responsive functional groups on SWCNTs plays an important role in tuning the conductance of different pH buffers. Furthermore, the proximal ion effect has been studied in this work by employing wPEs with amino groups possessing different pK_a values to control the ability to capture hydrogen ions in the vicinity of SWCNTs.

AUTHOR INFORMATION

Corresponding Author

*E-mail: tcui@me.umn.edu. Tel: 612-626-1636.

ACKNOWLEDGMENT

This work was partially supported by the DARPA M/NEMS Science and Technology Fundamentals Program through the Micro/nano Fluidics Fundamentals Focus (MF3) Center. We acknowledge the Nanofabrication Center, University of Minnesota, which is supported by the NSF through NNIN. Part of this work was carried out in the Characterization Facility, University of Minnesota.

REFERENCES

(1) Iijima, S. *Nature* **1991**, *354*, 56–58.
(2) Snow, E. S.; Perkins, F. K.; Houser, E. J.; Badescu, S. C.; Reinecke, T. L. *Science* **2005**, *307*, 1942–1945.
(3) Sotiropoulou, S.; Chaniotakis, N. *Anal. Bioanal. Chem.* **2003**, *375* (1), 103–105.
(4) Fennimore, A. M.; Yuzvinsky, T. D.; Han, W.-Q.; Fuhrer, M. S.; Cumings, J.; Zettl, A. *Nature* **2003**, *424*, 408–410.
(5) Chen, Z.; Appenzeller, J.; Lin, Y.-M.; Sippel-Oakley, J.; Rinzler, A. G.; Tang, J.; Wind, S. J.; Solomon, P. M.; Avouris, P. *Science* **2006**, *311*, 1735.
(6) Hierold, C.; Jungen, A.; Stampfer, C.; Helbling, T. *Sens. Actuators, A* **2007**, *136*, 51–61.
(7) Zhao, M.; Sharma, V.; Wei, H.; Birge, R. R.; Stuart, J. A.; Papadimitrakopoulos, F.; Huey, B. D. *Nanotechnology* **2008**, *19*, 235704.
(8) Kwon, J.-H.; Lee, K.-S.; Lee, Y.-H.; Ju, B.-K. *Electrochem. Solid-State Lett.* **2006**, *9*, H85–H87.
(9) Kim, S.; Yim, J.; Wang, X.; Bradley, D. D.; Lee, S.; deMello, J. C. *Adv. Funct. Mater.* **2010**, *20*, 2310–2316.
(10) Li, X.; Zhang, L.; Wang, X.; Shimoyama, I.; Sun, X.; Seo, W.-S.; Dai, H. *J. Am. Chem. Soc.* **2007**, *129*, 4890–4891.
(11) Choi, S.-W.; Kang, W.-S.; Lee, J.-H.; Najeeb, C. K.; Chun, H.-S.; Kim, J.-H. *Langmuir* **2010**, *26*, 15680–15685.
(12) Decher, G. *Science* **1997**, *277*, 1232–1237.
(13) Rouse, J. H.; Lillehei, P. T. *Nano Lett.* **2002**, *3*, 59–62.
(14) Lee, D.; Cui, T. *IEEE Sens. J.* **2009**, *9*, 449–456.
(15) Loh, K. J.; Kim, J.; Lynch, J. P.; Kam, N. W. S.; Kotov, N. A. *Smart Mater. Struct.* **2007**, *16*, 429–438.
(16) Xue, W.; Cui, T. *Sens. Actuators, B* **2008**, *134*, 981–987.
(17) Yu, X.; Rajamani, R.; Stelson, K. A.; Cui, T. *Sens. Actuators, A* **2006**, *132*, 626–631.
(18) Gong, K.; Yan, Y.; Zhang, M.; Su, L.; Xiong, S.; Mao, L. *Anal. Sci.* **2005**, *21*, 1383–1393.
(19) Hesketh, T. R.; Moore, J. P.; Morris, J. D. H.; Taylor, M. V.; Rogers, J.; Smith, G. A.; Metcalfe, J. C. *Nature* **1985**, *313*, 481–484.
(20) Back, J. H.; Shim, M. *J. Phys. Chem. B* **2006**, *110*, 23736–23741.
(21) Kaempgen, M.; Roth, S. *J. Electroanal. Chem.* **2006**, *586*, 72–76.
(22) Yang, C. F.; Chen, C. L.; Busnaina, A.; Dokmeci, M. R., Single-Walled Carbon Nanotube Based pH Sensors on a Flexible Parylene-C substrate. In *Proceedings of the Annual Conference of the IEEE Engineering in Medicine and Biology Society*; Institute of Electrical and Electronics Engineers: New York, 2009; pp 4102−4105.
(23) Ferrer-Anglada, N.; Kaempgen, M.; Roth, S. *Phys. Status Solidi B* **2006**, *243*, 3519–3523.
(24) Zhao, L.; Nakayama, T.; Tomimoto, H.; Shingaya, Y.; Huang, Q. *Nanotechnology* **2009**, *20*, 325501.
(25) Lee, D.; Cui, T. *J. Vac. Sci. Technol., B* **2009**, *27*, 842–848.
(26) Liu, J.; Rinzler, A. G.; Dai, H.; Hafner, J. H.; Bradley, R. K.; Boul, P. J.; Lu, A.; Iverson, T.; Shelimov, K.; Huffman, C. B.; Rodriguez-Macias, F.; Shon, Y.-S.; Lee, T. R.; Colbert, D. T.; Smalley, R. E. *Science* **1998**, *280*, 1253–1256.
(27) Bhatia, S. R.; Khattak, S. F.; Roberts, S. C. *Curr. Opin. Colloid Interface Sci.* **2005**, *10*, 45–51.
(28) Xue, W.; Cui, T. *Nanotechnology* **2007**, *14*, 145709.
(29) Elzbieciak, M.; Kolasinska, M.; Warszynski, P. *Colloids Surf., A* **2008**, *321*, 258–261.
(30) Wong, S. S.; Joselevich, E.; Woolley, A. T.; Cheung, C. L.; Lieber, C. M. *Nature* **1998**, *394*, 52–55.